

PREDICTION OF 3D INDOOR AIRFLOW-RADIATION INTERACTIONS BY DISCRETE TRANSFER METHOD

Yuguo Li, Laszlo Fuchs
Department of Gasdynamics
The Royal Institute of Technology
S-100 44 Stockholm SWEDEN

ABSTRACT

Scaling parameters are presented for the interaction of surface and/or gas radiation in indoor air flow problem. These are used together with experimental results to indicate that the surface radiation has a considerable effect in some buoyancy controlled ventilated rooms. The effects of gas radiation are discussed.

The discrete transfer method (DTM) has been coupled with our indoor flow code which is used to solve some flow problems. The computer storage for radiation calculation is smaller and complex geometries as well as shadows can be easily treated. The discrete equations are solved by multi-grid iterations. We study the accuracy of surface radiation prediction as compared to a conventional radiation model using shape factor. For prescribed sources in a 3D enclosure, we consider the accuracy of the model as compared to Monte Carlo methods. Lastly, natural convection and radiation interactions in a 3D enclosure are simulated numerically. Characteristics of the flow and temperature fields are compared with other published results and are found to be in rather good agreement.

THE HISTORY OF THE UNITED STATES OF AMERICA

CHAPTER I
THE EARLY PERIOD
1492-1600

The first European settlement in North America was established by Christopher Columbus in 1492. The Spanish explorer sailed across the Atlantic Ocean and landed on the island of Hispaniola. He then sailed to the mainland and established a settlement at San Salvador. The Spanish continued to explore and settle in North America, with Juan Ponce de Leon discovering Florida in 1513. The English first arrived in North America in 1482, when John Cabot sailed from England to the coast of North America. The English established a settlement at Roanoke in 1585, but it was abandoned in 1586. The Pilgrims arrived in North America in 1620, and established the Plymouth Colony. The Puritans arrived in North America in 1630, and established the Massachusetts Bay Colony. The French explored and settled in North America, with Jacques Cartier discovering the Gulf of St. Lawrence in 1498. The French established a settlement at Quebec in 1608. The Dutch explored and settled in North America, with Henry Hudson discovering the Hudson River in 1609. The Dutch established a settlement at New Amsterdam in 1614. The Swedish explored and settled in North America, with Peter Minuit establishing the colony of New Sweden in 1638. The Dutch and Swedish colonies were eventually absorbed into the British Empire.

THE EARLY PERIOD

The early period of American history is characterized by exploration and settlement. The Spanish, English, French, Dutch, and Swedish all explored and settled in North America. The Spanish established the first permanent European settlement in North America at St. Augustine in 1565. The English established the first permanent English settlement in North America at Jamestown in 1607. The Pilgrims established the first permanent English settlement in New England at Plymouth in 1620. The Puritans established the first permanent English settlement in New England at Boston in 1630. The French established the first permanent French settlement in North America at Quebec in 1608. The Dutch established the first permanent Dutch settlement in North America at New Amsterdam in 1614. The Swedish established the first permanent Swedish settlement in North America at New Sweden in 1638. The early period of American history was a time of great discovery and exploration.

PREDICTION OF 3D INDOOR AIRFLOW-RADIATION INTERACTIONS BY DISCRETE TRANSFER METHOD

Yuguo Li, Laszlo Fuchs

Department of Gasdynamics
The Royal Institute of Technology
S-100 44 Stockholm SWEDEN

INTRODUCTION

Over the past twenty years, more and more attention is being focused on the numerical simulation of air flows in buildings. The problem of indoor air flow has usually been simplified to study of enclosures which have boundaries of prescribed temperature or prescribed heat flux. This simplification is partly due to focusing on understanding the internal convective transport, and partly due to computational difficulties associated with accurate radiative heat transfer calculations. Previous work on coupling convection and surface/gas radiation has been reviewed in [1, 2]. The literature review shows degree of indeterminacy remains with respect to model accuracy, due to limited amount of experimental data for convection-radiation interactions[2]. Measured vertical temperature velocity profiles in a full-scale test room with displacement ventilation have been provided recently[3].

In this paper, the scaling parameters and some of the experimental results will be first presented to show why and when the radiative effects are considerable, following by a critical but brief review of the simplified methods for radiation calculation. The discrete transfer method is coupled with a multi-grid CFD code. The calculated results are compared with published results found in the literature.

When Is Radiation Considerable ?

The boundary conditions for the indoor air temperature are less obvious at radiating walls, i.e. not always of Dirichlet or Neumann types. Thermal boundary condition at the wall-air interface is usually unknown a priori. What we can assume to be known is the outdoor environment, which gives rise to a conjugate problem that includes the indoor air domain and the room wall domain. Distribution of temperature at the wall-air interface generally depends on the heat conduction through the wall, the thermal convection near the wall surface and the radiation between different surfaces. For sunlit surfaces, glazing surfaces, the situation is even more complex as shown schematically in Fig.1. For a general surface i in a room of N small isothermal grey surfaces with equal-area, the heat balance equation becomes,

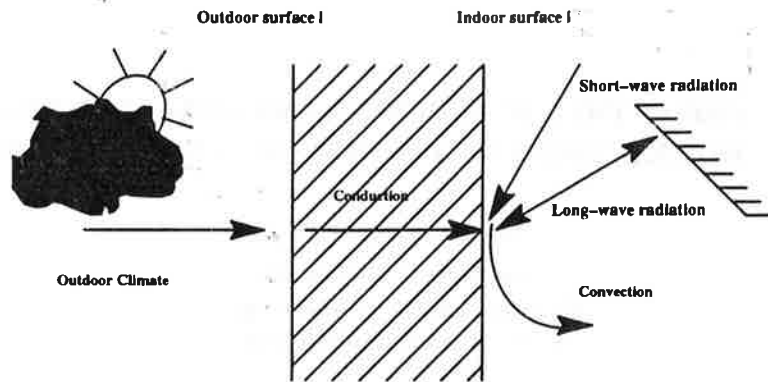


Fig.1 Thermal transport elements at an indoor surface i .

$$q_i = \lambda \frac{\partial T}{\partial n} + q_{r,w} \quad (1.1)$$

$$q_i = \lambda \frac{\partial T}{\partial n} + \sigma \epsilon T_{wi}^4 - \sigma \epsilon \sum_{j=1}^N G_{ji} T_{wj}^4 \quad (1.2)$$

Eq.(1.1) is a general expression of gas radiation case, whereas eq.(1.2) is specially valid for the case where only surface radiation is taken into account. Eq.(1.2) can be non-dimensionalized. The detailed derivation is given elsewhere[3].

Forced convection case:

$$q_i^* = \frac{1}{Pr Re} \frac{\partial T^*}{\partial n^*} + \frac{1}{Pl_s Pr Re} \sum_{j=1}^N F_{ij}^* (T_{wi}^* - T_{wj}^*) \quad (2)$$

Natural convection case:

$$q_i^* = \frac{1}{Nu} \frac{\partial T^*}{\partial n^*} + \frac{1}{Pl_s Nu} \sum_{j=1}^N F_{ij}^* (T_{wi}^* - T_{wj}^*) \quad (3)$$

A typical value of Pl_s is of order of -2 in an ordinary room. Eqs. (2) and (3) show that the scaling parameter that estimates the radiative effect is $1/(Pl_s Nu)$ (comparing radiation to convection) or $1/(Pl_s Re)$ (comparing radiation to heat transported by the ventilation air). The numbers $1/(Pl_s Re)$ or $1/(Pl_s Nu)$ may become larger at mixed convected or natural convected surfaces in non-isothermal mixing ventilation, specially with a low supply flow rate. The radiation plays a considerable role in the temperature distribution. It is mainly this radiation effect which makes that the maximum temperature range in the room air is always less than that between the extract and the supply. The temperature profiles in a black painted room and an aluminium coated room with displacement ventilation (room size $3.6 \times 4.2 \times 2.75 \text{ m}^3$) are shown in Fig.2. The wall surface temperature presented here is an average of the four walls. The profiles with different walls are not alike in spite of the fact

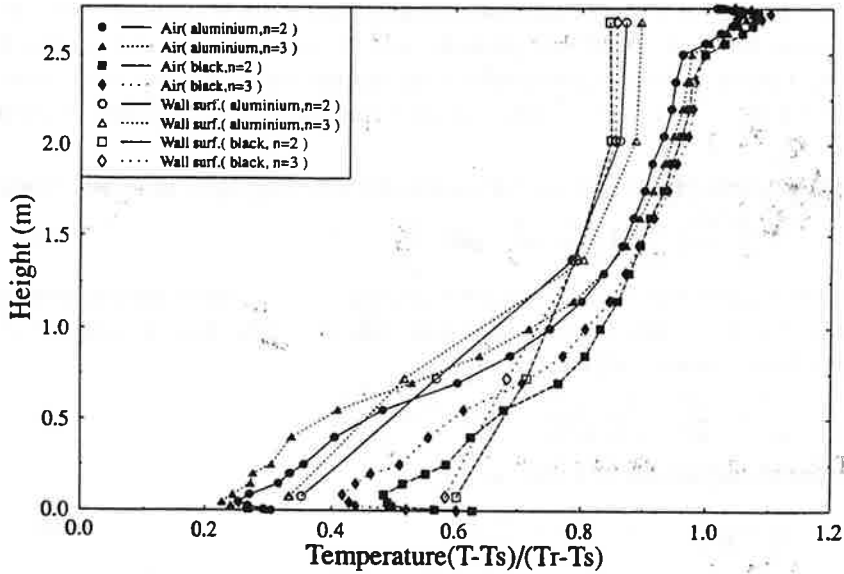


Fig.2 Vertical temperature profiles with aluminium wall cases and black wall cases for different supply flow rates (n). The heat load is 300W.

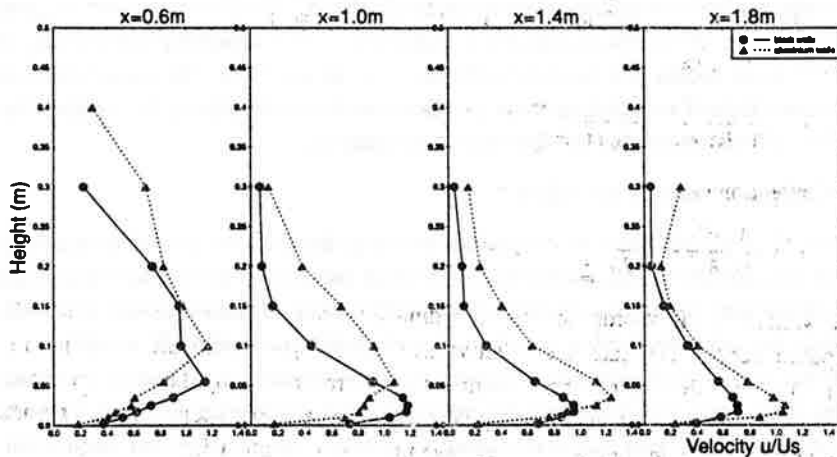


Fig.3 Mean streamwise velocity profiles near the floor at different distances X from the supply terminal. The heat load is 450W and the specific supply flow rate is 3 room volumes per hour.

that they are generated by the same heat source. An explanation to this difference is that much less heat is transported by radiation with aluminium walls. The floor surface heated by radiation from the ceiling will gradually heat the gravity current and weaken the buoyancy force in it. Some measured velocity profiles are displayed in Fig.3. The value of $1/(Pl_g Re)$ at the surface near the supply is much larger in displacement than in mixing ventilation.

When the air participates in the radiative heat transfer, the energy equation for air becomes,

$$\rho C_p \frac{\partial T}{\partial \tau} + \rho U_j \frac{\partial T}{\partial x_j} = \lambda \frac{\partial^2 T}{\partial x_i \partial x_i} + \frac{\partial}{\partial x_j} (-\rho \bar{u}_j T) + \frac{\partial q_{rj}}{\partial x_j} \quad (4)$$

The equation can be non-dimensionalized by dividing the variables by the corresponding reference length H_0 , velocity U_s , temperature difference ΔT_0 , time $\tau_0 (=H_0/U_s)$ and radiative flux $q_{r0} (=4\sigma T_0^3 \Delta T_0 \kappa H_0)$, we obtain,

$$\frac{\partial T}{\partial \tau} + U \frac{\partial T}{\partial x_j} = \frac{1}{Pr Re} \frac{\partial^2 T}{\partial x_i^2 \partial x_i^2} + \frac{\partial}{\partial x_j} (-u_j \bar{T}) + \frac{4}{Bo} \frac{\partial q_{rj}}{\partial x_j} \quad (5)$$

The Boltzman number can be written as

$$\frac{4}{Bo} = \frac{\tau}{Pl Pr Re} \quad \text{or} \quad \frac{4}{Bo} = \frac{1}{Pl_g Pr Re} \quad (6)$$

It should be noted that the definitions of the Planck (Pl) and Boltzman (Bo) numbers are different in the literature. The modified Planck number Pl_g gives the ratio between the conduction and the gas radiation. The higher absorption coefficient corresponds to larger optical thickness and smaller modified Planck number. Whether the gas radiation effect is large or not depends on the values of $1/(Pl_g Re)$. From the results of the formula in [4] for estimating the mean emittance of air from the mean geometrical path length and water vapor density, we find that the optical thickness in a $3.6*4.2*2.75 \text{ m}^3$ room is in the range of 0.0–0.03. From the above discussions, gas radiation is expected to be only considerable in the case of large rooms and humid conditions (e.g. in summer). The observation of considerable effects of air radiation in a convective heated room in [5] may be explained by the weaker convection comparing with mixing ventilation.

How to Calculate Surface Radiation ?

The choice of a particular method for radiation exchange depends not only on its accuracy and efficiency, but also on its conformity. Methods of analyses of the radiative exchange within a diffuse grey surface enclosure are not new. Two classical approaches are available, i.e. Poljak's net radiation method and Gebhart's absorption method[6]. If we divide the room surface into N small elements, we have a non-linear system of equations involving 4th power of unknown temperatures to determine the N sub-surface temperatures. This has been considered to be very time-consuming to solve in the cooling load calculation. Different so called radiant interchange algorithms have been introduced, see reviews and comparisons of these algorithms[4,7,8]. One common source of errors in these algorithms is the linearization, which is in general very small because of moderate temperature variations. The most important error is due to the non-uniform distribution of wall surface temperature. The remedy is to divide each wall to more sub-surfaces. This calls for an efficient method to calculate the shape factor F_{ij} and to solve the resulted system of

equations. It may be concluded that to employ existing load codes to supply the radiative boundary conditions, an efficient shape factor calculation method is required. Obviously, to ensure the accuracy, the load code must be modified to consider the air temperature distribution in the room.

Analytical, tabular, or graphical values of F_{ij} have been given for only few, relatively simple geometries. A general way for calculating F_{ij} is using numerical integration. Different ways, in which the integration is carried out, have been developed. These can be classified as Monte Carlo method, projected contour method, projection method, and the double area method. These methods have been compared in [9,10]. Several published FORTRAN programs or explicit expressions for the shape factor exist in the literature[11–13].

How to Calculate Gas Radiation ?

Different methods like zonal methods, statistical methods, flux methods, finite-element methods and hybrid methods have been reviewed in [2,14]. The basic flaw of the zonal method is the computational effort required to calculate the exchange factors between various volume and surface elements in complex geometries. This difficulty can be overcome using the Monte Carlo method to calculate the direct exchange areas. The Monte Carlo method suffers from statistical error as well as the extensive computational time. If the direction of each ray is given deterministically, then the computations are simplified. This is the idea of Discrete Transfer Method(DTM) which combines the virtues of the zonal, Monte Carlo and the flux methods[14]. Here we use the DTM.

GOVERNING EQUATIONS

The room air is in general not a scattering medium. We consider a three-dimensional ventilated room which contains absorbing-emitting grey air. All the inside wall surfaces are considered to be grey and diffuse. The conservation equations take a general form

$$\frac{\partial(\rho\phi)}{\partial\tau} + \frac{\partial}{\partial x_i}(\rho U_i - \Gamma_\phi \frac{\partial\phi}{\partial x_i}) = S_\phi \quad (7)$$

The dependent variable ϕ takes the forms of U , V , W , T , k , ϵ , and 1(for the continuity equation). Standard high-Reynolds number k - ϵ turbulence model with wall functions have been employed. The specified boundary conditions and the corresponding coefficients Γ_ϕ and sources S_ϕ can be found in [15]. The boundary condition for the energy equation (4) is the heat balance eq.(1.1).

The radiation transfer equation (RTE), which represents the change in the intensity dl for a ray travelling distance ds through an absorbing-emitting medium is

$$\frac{dl}{ds} = -\kappa l + \frac{\kappa\sigma T^4}{\pi} \quad (8)$$

The net radiative heat flux in eq.(1.1) can be obtained by subtracting the leaving flux $q_{r,w}^+$ from the arriving flux $q_{r,w}^-$.

$$q_{r,w} = \int_{2\pi} I^+ d\Omega - \int_{2\pi} I^- d\Omega \quad (9)$$

The radiative source term in eq.(4) is equivalent to the net outflow of radiant energy per unit volume, which can be obtained by integrating eq.(8) over the entire solid angle 4π .

$$\frac{\partial q_r}{\partial x} + \frac{\partial q_r}{\partial y} + \frac{\partial q_r}{\partial z} = 4\kappa\sigma T^4 - \kappa \int I d\Omega \quad (10)$$

Eq.(8) depends on the local temperature, radiative intensity and the integral with respect to the solid angle in eq.(9) and eq.(10), this brings the enclosure geometry and all its complexity into the calculation. An additional boundary conditions, which describes how the radiation is being exchanged at the radiating boundaries, is required for the radiation transfer equation, i.e.,

$$q_{r,w}^+ = (1 - \epsilon) q_{r,w}^- + \sigma \epsilon T_w^4 \quad (11)$$

It should be noted that when the air is considered as transparent, eq.(11) determines only the surface radiation exchange, which can be determined alternatively by the classical net radiation method or Gebhart's absorption method.

NUMERICAL METHODS

The physical domain is discretized with a global uniform rectangular mesh. In regions of high gradients, e.g. near wall regions and at inlet/outlet regions, locally refined meshes can be added. The diffusive term is approximated by central differences. The convective terms are approximated by the hybrid central/upwind differencing scheme. The discretized equations are solved by a multi-grid procedure[15,16].

The radiative transfer equation is solved by the DTM[14]. The physical domain is discretized on a rectangular mesh, see Fig.4. It does not necessarily be the same as used in flow calculation. The hemisphere about the boundary point P_i is divided into $N = N_\theta * N_\phi$ equal segments, where N_θ and N_ϕ are corresponding to polar angle θ and azimuthal angle ϕ . Each subdivision is then $d\theta = \pi / (2N_\theta)$ and $d\phi = 2\pi / (N_\phi)$. We first initialize the leaving flux at each boundary point, then determine the intensities along each ray in the reverse direction towards P_i from the recurrence relation, which is obtained by integrating the radiation transfer equation along a ray distance s .

$$I_{s+1} = \frac{\sigma T^4}{\pi} (1 - \epsilon^{w}) + I_s \epsilon^{w} \quad (12)$$

The arriving flux $q_{r,w}^-$ for each boundary point is calculated by summing over all the impinging intensities for the whole hemisphere. The leaving flux $q_{r,w}^+$ is then obtained by eq. (11). If the walls are not black, the value of $q_{r,w}^+$ is dependent on $q_{r,w}^-$. Iterations are required until the absolute change in $q_{r,w}^+$ is less than a prescribed small value. The amount of energy "left" behind by the rays as they traverse each cell is accumulated to obtain the radiation source term.

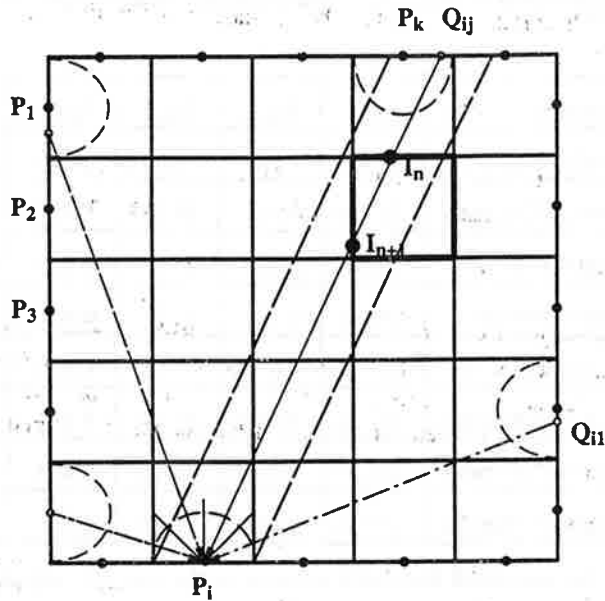


Fig.4 Illustration of the idea behind the discrete transfer method.

Two assumptions have been made in the sum of the radiative source term and the sum of the wall fluxes. The leaving flux at Q_j is assumed to be equal to the leaving flux at the boundary point which lies on the same boundary cell. The effect of partial overlapping between the control volume of the cell and the ray is neglected. These can be overcome by refining the grid and the ray.

In gas radiation interaction problems, the radiation source terms and boundary radiation fluxes are calculated after the temperature field is determined which then provides the input to the energy equation for the next iteration. For a steady state solution, one does not necessarily update these variables in each iteration.

RESULTS AND DISCUSSIONS

Primary Evaluations

The code is firstly evaluated for the buoyant flow calculations and radiation calculations, respectively. The numerical results in a square with side walls at different constant temperatures, and with insulated floor and ceiling, are presented in Table 1. The most reliable benchmark solutions [17] are used for comparison. Good agreement at different Rayleigh numbers (10^3 , 10^4 , 10^5 and 10^6 , not all shown in the Table 1) has been found. The results also show that grid refinement improves the prediction.

The radiation calculation is evaluated with the results from the Monte Carlo method. The test case has been evaluated in [14]. The purpose here is to study the effect of ray

Table 1. Comparisons of velocity fields and convection heat transfer coefficients.

Ra	Results	W_{max}	X_{wmax}	U_{max}	Z_{umax}	Nu_0
10^4	de Vahl Davis [17]	19.617	0.119	16.178	0.823	2.238
	Present 20*20 mesh	19.748	0.119	16.281	0.822	2.431
	Present 40*40 mesh	19.623	0.120	16.217	0.823	2.307
	Present 80*80 mesh	19.522	0.120	16.223	0.821	2.270
10^6	de Vahl Davis [17]	219.36	0.0379	64.63	0.850	8.817
	Present 20*20 mesh	234.32	0.0250	69.90	0.882	10.27
	Present 40*40 mesh	221.77	0.0395	71.16	0.865	10.21
	Present 80*80 mesh	217.46	0.0411	70.23	0.857	9.567

where U_{max} is the maximum horizontal velocity on the vertical mid-plane; Z_{umax} is its location; W_{max} is the maximum vertical velocity on the horizontal mid-plane; X_{wmax} is its location; Nu_0 is the average Nusselt number on the vertical boundary.

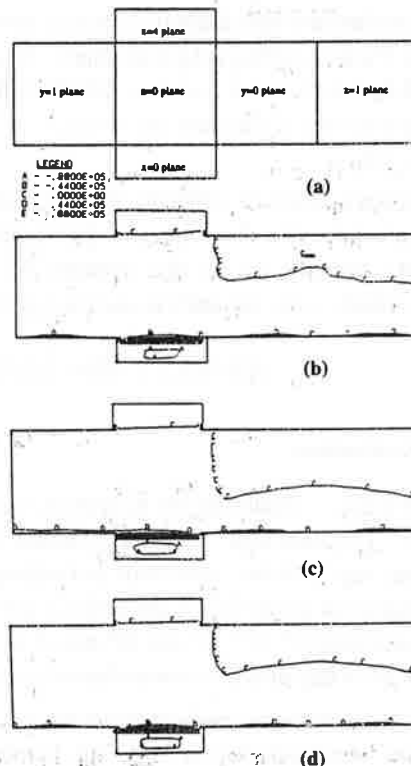


Fig. 5 The net flux through six walls, (a) six walls; (b) Monte Carlo; (c) DTM(4*4 rays); (d) DTM(32*32 rays).

refinement. The case is a 4m*1m*1m rectangular enclosure. The gas inside is in thermal equilibrium in the absence of conduction and convection effects. The gas absorption coefficient is 0.2 1/m. All the walls are black and their temperatures are at $X=0$, $T_w=1200K$; at $X=4$, $Y=0$, $Z=1$, $T_w=300K$ and at $Y=1$, $Z=0$, $T_w=50K$. A 16*4*4 uniform mesh is used, with two different rays, 4*4 and 32*32, respectively. The net flux through six walls is shown in Fig.5. Clearly, the finer ray we have, the better results we achieve.

Surface Radiation Calculation Using DTM

DTM can be used to calculate the shape factors[14]. For a given sub-surface, a mesh is generated so that none of the grid cell subtends an exceptionally large solid angle at the sub-surface at which the shape factor is being calculated. The required integrals are then discretized and summed. The resulted shape factors are then stored. The main problem is that the memory required to store those shape factors is proportional to the square of the number of the sub-surfaces. An alternative way is to obtain the radiative flux at the wall surfaces by using existing scheme of DTM with zero optical thickness. No shape factors are needed to be stored. To study the accuracy of the method, we derive the equivalent shape factor calculated by DTM. The shape factor F_{12} is defined by the fraction of the energy leaving black surfaces A_1 that arrives at black surface A_2 . The total energy leaving the black surface A_{Pk} , which is assumed as A_{Qij} , is $I_0\pi A_{Pk}$. The radiation leaving A_{Pk} that reaches A_{Pi} is $\sum I_0(\sin\theta\cos\theta)(\sin d\theta)d\phi A_{Pi}$. So the F_{ki} can be calculated as

$$F_{ki} = \frac{(\sin\theta \cos\theta)(\sin d\theta)d\phi A_{Pi}}{\pi A_{Pk}} \quad (13)$$

We model an empty rectangular room 4.8m long by 2.4m wide by 2.4m high. A 8*4*4 uniform mesh is used, and this gives $N=160$ elements. The shape factors calculated with different rays are compared in Fig.6 with those calculated by the subroutine in two-band radiation model[1]. Only the shape factors between an element of floor and the elements of ceiling are presented. The radiative energy conservation is checked by comparing $\sum F_{ij}$ from $j=1$ to N in Fig. 7. Figs. 6 and 7 show that less rays give rise to large errors. The imbalance of the total energy is about 10% in this test case. This phenomena has also been observed when the gas radiation is considered in a 3D enclosure[14]. In spite of this, the DTM gives an economical way for applying the general thermal boundary conditions in indoor air flow simulation.

Interaction of Natural Nonvection and Gas Radiation

We further examine radiation-convection interactions in a cube filled with grey gas and heated differently by two vertical walls(Fig.8). The remaining walls are thermally insulated. All the inner surfaces are assumed to be black. The absorption coefficient is 0.2 1/m, which means optical thickness is 0.2L, where L is the side of the cube. The Rayleigh number is $5*10^5$. The temperatures of the cooled and heated walls are 275K and 285K, respectively. The Prandtl number is 0.7. Consequently, the side of the cubic is .18m and the modified Planck number is about 30. The calculations have been performed with 40*40*40 uniform grids and 4*4 rays. The temperature field at vertical mid-plane ($y=0.5L$) is shown in Fig.9. The field is symmetric when the radiation is absent due to the Boussinesq


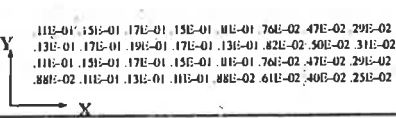
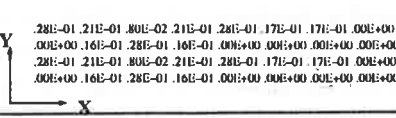
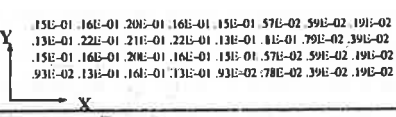
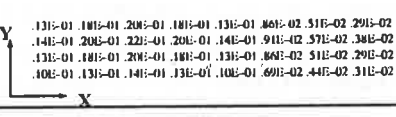
<p>A sub-surface at floor</p>	
<p>Two-band Radiation Model</p>	
<p>DTM 10*10 Rays</p>	
<p>DTM 30*30 Rays</p>	
<p>DTM 100*100 Rays</p>	

Fig.6 The shape factors between a sub-surface at floor and all the sub-surfaces at ceiling.

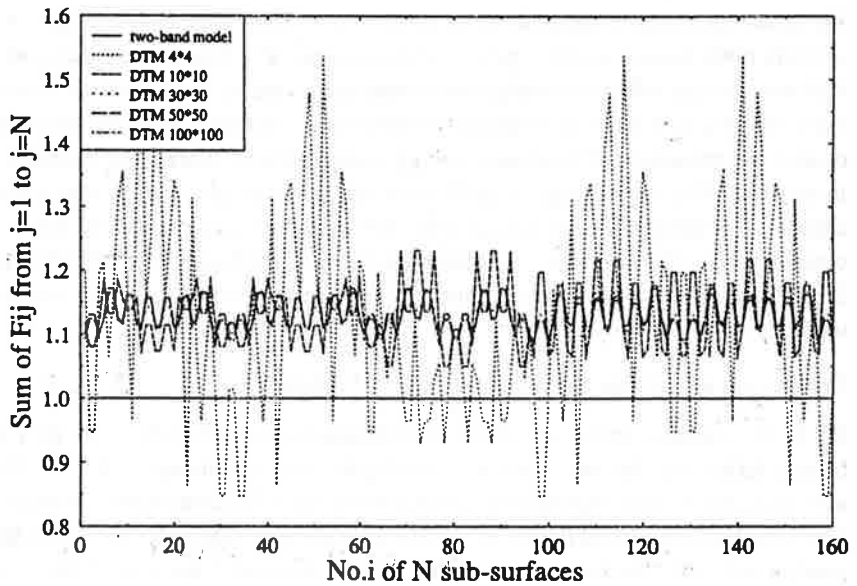


Fig.7 The sum of F_{ij} from $j=1$ to N for different sub-surfaces i in a room. F_{ij} is calculated by different methods.

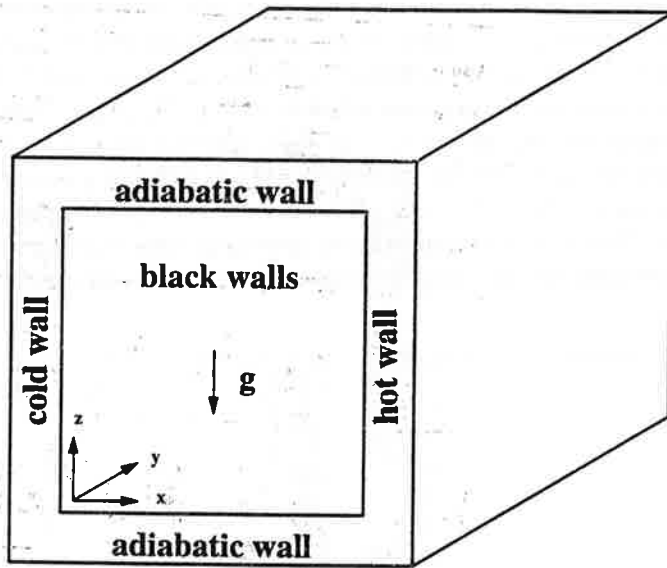


Fig.8 A 3D cubic enclosure.

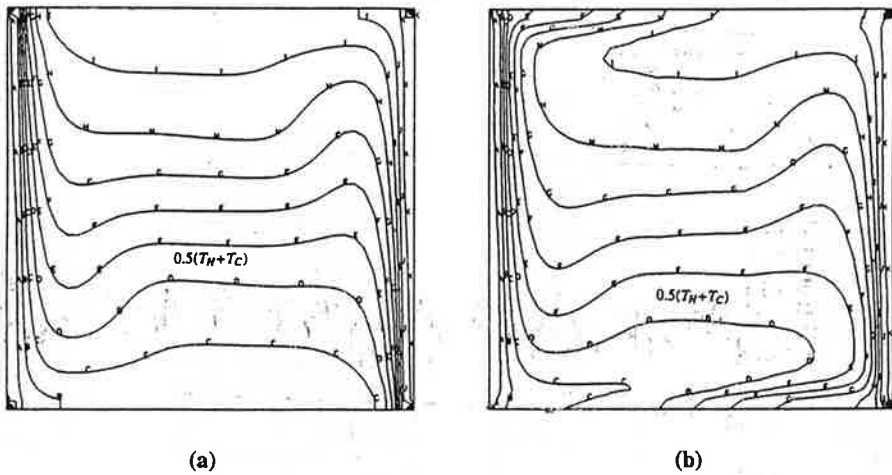


Fig.9 The temperature fields at vertical mid-plane, (a) natural convection; (b) natural convection+gas radiation.

approximation, but this symmetry does not exist any longer when the radiation is taken into account. The core region becomes warmer which can be seen from the downwards shift of the average temperature $0.5(T_H+T_C)$ isotherm. The temperature gradients of the floor and the ceiling are no longer zero due to surface radiation exchange. The temperature fields at horizontal mid-plane ($z=0.5L$) are shown in Fig.10a-b. Large variation of temperature in the heated half can be observed due to gas radiation. The corresponding velocity field is shown in Fig.10c-d. The symmetry is lost again due to the corresponding change in the temperature field. These results are in good agreement with the numerical study of Fusegi et al[18]. They consider flows in cubical enclosures filled with nongray gas (CO_2).

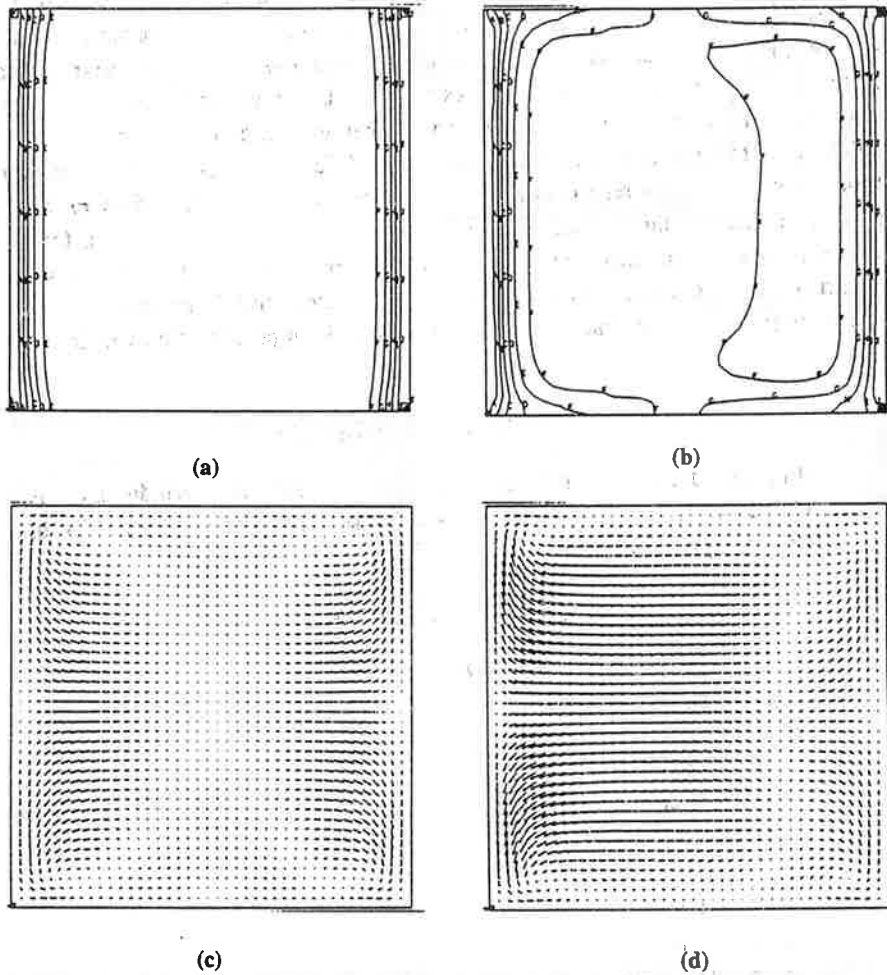


Fig.10 The temperature fields at horizontal mid-plane, (a) natural convection; (b) natural convection+gas radiation; the velocity fields at horizontal mid-plane, (c) natural convection,, (d) natural convection+gas radiation.

The effect of gas radiation is to provide more uniform gas temperature in the enclosure. The effect obviously depends on the absorbance of the particular gas considered. In room case, the air emittance is much lower than those in previous studied and the temperature difference between indoor surfaces are also much smaller. Whether the above conclusions can be applied in room case requires further study. The radiation calculation method and coupling approach developed here provide a numerical tool for such future study

CONCLUSIONS

We attempt to provide tools to gain more understanding of the radiative effects on air flow. The effect of surface radiation is considerable in some non-isothermal ventilated room, especially in buoyancy controlled displacement ventilated rooms. The gas radiation effects is probably important in large enclosures and summer conditions. More research is required to further identify when or whether the gas radiation is considerable due to the lower absorption coefficient of room air. Different radiation algorithms in cooling loads calculation, different shape factor algorithms and different gas radiation calculation methods are reviewed with respect to accuracy, efficiency and conformity with CFD code. A general thermal boundary conditions and a coupling approach are specified for the radiation-convection interaction problem. The discrete transfer method is coupled with a multi-grid CFD solver to study the 3D radiation-airflow interaction. The radiation is found to alter significantly the characteristics of the flow and temperature fields in the case studied.

ACKNOWLEDGEMENT

The first author would like to thank Dr. Sture Holmberg and Prof. Mats Sandberg for their interests and discussions in this work. The work was financially supported by the Swedish Council for Building Research (BFR).

LIST OF SYMBOLS

B_0	Boltzman number $\rho c_p U_s / (\sigma T_0^3 \kappa H_0)$
c_p	specific heat of air at constant pressure (Ws/KgK)
F	shape factor
G_{ij}	Gebhart's absorption factor
h	convective heat transfer coefficient (W/m ² K)
I	radiative intensity (W/m ² sΩ)
n	normal direction of wall surface
Nu	Nusselt number hH_0/λ
Pr	Prandtl number $\mu c_p/\lambda$
Pl_s	Surface Planck number $\lambda/(4T_0^3 H_0 \epsilon \sigma)$
Pl_g	Gas Planck number $\lambda/(4T_0^3 H_0^2 \kappa \epsilon \sigma)$
Pl	Planck number $\lambda/(4T_0^3 H_0 \sigma)$
q_i	heat rate conducted through wall to surface i (W/m ² K)
q_r	radiative flux (W/m ² K)

Re	Reynolds number $\rho U_s H_0 / \mu$
T	temperature (K)
t	fluctuating temperature (K)
u	fluctuating velocity (m/s)
U	velocity (m/s)
U_s	supply velocity (m/s)

Greek symbols

ϵ	emissivity of wall surface
ϕ	general variables
λ	thermal conductivity of air (W/mK)
κ	radiative absorption coefficients of air (1/m)
μ	dynamic viscosity of air (Kg/ms)
π	3.1415926
Ω	solid angle
τ	time (s)
$\bar{\tau}$	optical thickness κH_0
ρ	density of air (Kg/m ³)
σ	Stefan-Boltzman constant ($5.6697 \cdot 10^{-8} \text{W/m}^2 \text{K}^4$)

Superscript

*	dimensionless quantity
+	leaving flux
-	arriving flux

Subscript

w	quantity for wall
---	-------------------

REFERENCES

- [1] Li, Y., Fuchs, L.: "A two-band radiation model for calculating room wall temperature". Recent Development in Heat Transfer. Proceedings of First Baltic Heat Transfer Conference, Göteborg, Sweden, 26th-31st, August, 1991.
- [2] Yang, K.T.: "Numerical modelling of natural convection-radiation interactions in enclosures". Pro. 8th Int. Heat Transfer Conf., vol. I, pp.131-140, 1986.
- [3] Li, Y., Sandberg, M., Fuchs, L.: "Radiative effects on airflow with displacement ventilation: An experimental investigation". Submitted to Energy and Building, 1992.
- [4] Carroll, J.A.: "A comparison of radiant interchange algorithms". 3rd Annual Conference of Solar Engineering, Reno, April 27-May 1, 1981
- [5] Allard, F., Inard, C., Draoui, A.: "Influence of radiative participation of inside air on natural convection in a room". 12th AIVC Conference, Ottawa, Canada, 24-27 September, 1991.

- [6] Siegel, R. and Howell, J.R. "Thermal radiation heat Transfer". Hemisphere, 1981.
- [7] Stefanizzi, P., Wilson, A., Pinney, A. "Internal Longwave Radiation exchange in buildings: Comparison of calculation methods: I Review of algorithms". Building Serv. Eng. Res. Technol. 11(3) 81-85, 1990.
- [8] Stefanizzi, P., Wilson, A., Pinney, A. "Internal Longwave Radiation exchange in buildings: Comparison of calculation methods: II Testing of algorithms Building". Serv. Eng. Res. Technol. 11(3) 87-96, 1990.
- [9] Kadaba, P.V. "Thermal radiation viewfactor methods, accuracy and computer aided procedures". NASA/MSFC report, Contract NGT-01-002-099, 1982.
- [10] Emery, A.F., Johansson, O., Lobo, M., Abrous, A. "A comparative study of methods for computing the diffuse radiation view factors for complex structures". J. Heat Transfer, vol. 113, pp.413-422, 1991.
- [11] Mitalas, G.P., and Stephenson, D.G. "FORTRAN IV programs to calculate radiant interchange factors". NRC of Canada, Ottawa, Canada, DBR-25, 1966.
- [12] Gross, U., Spindler, K., and Habne, E. "Shape factor equation of radiation heat transfer between plane rectangular surfaces of arbitrary position and size with parallel boundaries". Letters in Heat and Mass Transfer, vol.8, pp.219-227, 1981.
- [13] Walton, G.N. "Algorithms for calculating radiation viewfactors between plane convex polygons with obstructions". NBSIR 86-3463, 1986.
- [14] Shah, N.G.: "New method of computation of radiation heat transfer in combustion chambers". Ph.D. thesis, Department of Mechanical Engineering, Imperial College of Science and Technology, London, 1979.
- [15] Li, Y., Fuchs, L., Holmberg, S.: "An evaluation of a computer code for predicting indoor airflow and heat transfer". Proceedings of 12th AIVC Conference, vol.3, pp.123-136, 1991.
- [16] Bai, X.S., Fuchs, L. "A fast multi-grid method for 3-D turbulent incompressible flows". To be published in Numerical Methods for Heat and Fluid Flow, 1992.
- [17] de Vahl Davis, G. "Natural convection of air in a square cavity: an accurate numerical simulation". Report 1981/FMT/1, School of Mechanical and Industrial Engineering, The University of New South Wales, Australia, 1981.
- [18] Fusegi, T., Ishii, K., Farouk, B., Kuwahara, K. "Natural convection-radiation interactions in a cube filled with a nongray gas". Numerical Heat Transfer, Part A, vol. 19, pp.207-217, 1991.

